Journal of Sol-Gel Science and Technology (2019) 89:29–36
https://doi.org/10.1007/s10971-018-4682-2

BRIEF COMMUNICATION: NANO AND MACROPOROUS MATERIALS (AEROGELS, XEROGELS, CRYOGELS, ETC.)

Synthesis of hierarchically porous MgO monoliths with continuous structure via sol–gel process accompanied by phase separation

Xuanming Lu[1] · Kazuyoshi Kanamori[1] · Kazuki Nakanishi[1]

Received: 22 February 2018 / Accepted: 7 May 2018 / Published online: 23 May 2018

Abstract

Hierarchically porous magnesium oxide, MgO, monoliths with a well-defined continuous macroporous structure have been synthesized via the sol–gel route accompanied by phase separation. Magnesium chloride hexahydrate was used as a precursor, and propylene oxide was used as an acid scavenger to raise the pH of a reaction solution homogenously. In order to obtain a crack-free monolith after heating in air, poly(vinylpyrrolidone), PVP, was employed as a scaffold of the skeleton as well as a phase separation controller to form the continuous macropores with higher homogeneity. Due to the moderate hydrogen-bonding interaction with magnesium hydroxide, PVP reinforces the gel network essentially composed of fine grained magnesium hydroxide. Even after the removal of all organic components by calcination, the porous gel samples maintained their monolithic form. On the other hand, an additional incorporation of 1,3,5-benzenetricarboxylic acid, H_3BTC, was found to be effective in suppressing the oriented growth of the micrometer-sized crystalline phase. The polycrystalline MgO monoliths with specific surface area of 185, 64, and 48 $m^2 g^{-1}$ were prepared after heating at 400, 500, and 600 °C in air, respectively.

Graphical Abstract

Appearances (upper) and SEM images(lower) of monolithic MgO-based gel before and after heat-treatment.

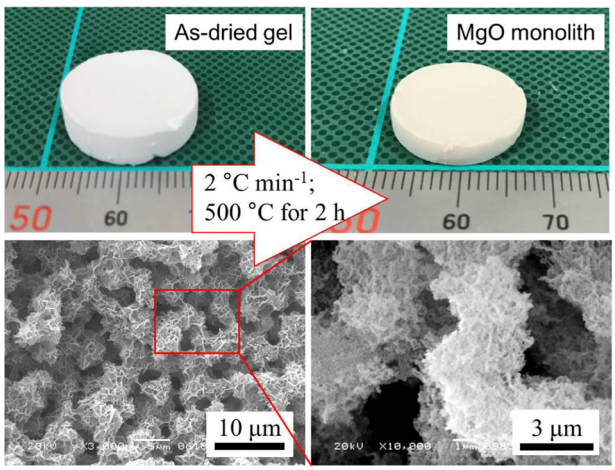

Pictures (upper) and SEM images (lower) of monolithic MgO-based gel before and after heat treatment

✉ Kazuki Nakanishi
kazuki@kuchem.kyoto-u.ac.jp

[1] Department of Chemistry, Graduate School of Science, Kyoto University, Kitashirakawa, Sakyo-ku, Kyoto 606-8502, Japan

Keywords Magnesium oxide · Sol–gel · Phase separation · Hierarchical pore structure · Monoliths

Highlights

- Hierarchically porous magnesium oxide (divalent metal oxide) monoliths with three-dimension network structure are synthesized.
- The network structure can be preserved after heat treatment under oxidative conditions.
- The fraction of pores larger than 30 nm can be controlled by addition of 1,3,5-benzenetricarboxylic acid.

1 Introduction

Hierarchically porous materials have been attracting keen attentions in the fields of energy conversion and storage [1], catalysis [2], separation [3], and adsorption [4]. The multiscale porous materials possess well-defined pores in discrete length-scales typically ranging from micro (<2 nm), meso (2–50 nm) to macro-pores (>50 nm). The continuous macropores provide the materials with high permeability, while the open mesopores and micropores contribute to enlarge the available surface area. Hierarchically porous monoliths integrating these properties offer advantages of recyclability, ease of separation, which are in general unavoidable problems with nanoparticles.

One of the commonly used methods to prepare hierarchically porous monoliths is the so-called sol–gel process. The sol-gel process offers advantages of broad applicable chemical compositions, mild reaction conditions, and versatility in preparing materials in various size and shapes. Nearly 30 years ago, Nakanishi and Soga successfully synthesized hierarchically porous silica, SiO_2, monoliths via the sol–gel process accompanied by phase separation [5]. In this method, macropores are formed via polymerization-induced phase separation, which are commonly recognized in organic polymer blends and multicomponent inorganic glasses. The driving force of phase-separation can be qualitatively explained by the Flory-Huggins formula [6, 7]. The sol–gel process proceeds simultaneously with the phase separation, and then freezes its transient structure including the co-continuous structure, which consists of two conjugate phases (solid gel-phase and fluidic sol-phase). The monolith with co-continuous solid skeletons and macropores can be obtained after a removal of the solvent-phase by washing and drying.

Based on the silica system, many hierarchically porous metal oxide monoliths have been successfully synthesized, such as titanium dioxide, TiO_2 [8, 9], zirconium dioxide, ZrO_2 [10], aluminum oxide, Al_2O_3 [11]. In the former two cases, a relatively high concentration of alkoxide precursors had to be employed to produce crack-free monoliths. Since the reactivity of alkoxides of titanium or zirconium is much higher than that of silicon alkoxide [12], it is necessary to suppress the reactivity of the alkoxides by an addition of chelating agents [9] or a careful control of solution pH [10] for a successful preparation of the oxide monoliths.

In 2001, Gash and co-workers used inorganic metal salts, instead of alkoxides, as precursors to synthesize iron (III) oxide [13] and aluminum oxide monoliths [14] in the form of supercritically dried aerogel. Epoxides as acid scavengers were added to the precursor solution to increase the solution pH uniformly, which drove the hydrolysis and polymerization of hydrated metal species to allow homogeneous gelation. Tokudome and co-workers introduced the polymerization-induced phase separation method to the above epoxide-mediated sol-gel system to produce hierarchically porous Al_2O_3 monoliths. Hierarchically porous iron-based [15], nickel-based [16], chromium-based [17], and copper-based [18] monoliths have also been synthesized through similar processes. In these cases, unlike alumina monoliths, the monolithic forms were not preserved after calcination under oxidative conditions. Due to the strong hydrogen-bond interaction between the metal (oxy) hydroxide oligomers and the phase-separation inducers such as poly(acrylic acid), HPAA, and poly(acrylamide), PAAm, the solid gel-phase obtained contains an appreciable fraction of organic components and only sparsely cross-linked inorganic components. Heat treatment under reducing atmosphere is an only way to preserve monolithicity and macroporous structure in the resultant calcined gels with fine carbon inclusions.

It is therefore still a challenge to prepare a single-phase crystalline metal oxide monolith in general with hierarchical pores in the sol–gel system accompanied by phase separation. Furthermore, it is more difficult for divalent metals to form monolithic oxides without the aid of structure-supporting components. Since the acidities of $[M(H_2O)_x]^{2+}$ complexes are much lower than those for metal aquo complexes with higher valence, the protonation of the added epoxide and resultant increase in pH of the solution will be suppressed. The slow hydrolysis/polycondensation tends to lead to precipitation rather than homogeneous gelation [16, 19].

In the present work, the preparation of magnesium oxide, MgO, monoliths with a co-continuous macroporous structure has been studied by the sol-gel process accompanied by phase separation. Poly(vinylpyrrolidone), PVP, was used both as a phase separation controller and a partial

mechanical support for the skeleton. Unlike the HPAA or PAAm-containing systems, PVP was found not to be a main component to mechanically support the monolithic form due to its weak interaction with metal hydroxide, and has relatively weak ability to suppress the condensation of Mg^{2+} aquo complexes compared to the cases with HPAA or PAAm. As a result, the degree of polycondensation in the Mg-based species will be high enough to maintain the monolithic form after the removal of organic components. In addition, 1,3,5-benzenetricarboxylic acid, H_3BTC, was employed to further suppress the nucleation and oriented growth, and to modify the meso- and micropore structures, which influenced on the specific surface area of the products. To the best of our knowledge, there is limited number of reports on the synthesis of the hierarchically porous monoliths with divalent metal oxides. The present work may provide a route to synthesize monolithic divalent metal oxides with appreciable specific surface area.

2 Experimental

2.1 Starting materials

Magnesium chloride hexahydrate ($MgCl_2{\cdot}6H_2O$, >98%), distilled water (H_2O), methanol (MeOH, >99.8 %), 2-propanol (IPA, >99%), and *n*-hexane (>99%) were purchased from Kishida Chemical Co., Ltd. (Japan). 1,3,5,-benzenetricarboxylic acid (H_3BTC, >98%) was purchased from Tokyo Chemical Ind. Co., Ltd. (Japan). Poly(vinylpyrrolidone) (PVP, $M_w = 10000$) and propylene oxide (PO) were purchased from Sigma-Aldrich Japan. All the agents were used without further purification.

2.2 Preparation of gel samples

The typical synthesis procedure for the monolithic Mg-based gel is as follows. 2 mmol of $MgCl_2{\cdot}6H_2O$ was dissolved in an aqueous methanol solution homogeneously, followed by an addition of 0.16 g of PVP. Then the solution was heated up to 50 °C for 20 min to accelerate the dissolution of PVP. After cooling the solution down to room temperature, 0.28 mL of PO was injected into the solution under stirring, followed by stirring for 1 min. The solution was tightly sealed and placed in a constant temperature oven at 25 °C for gelation. In the case of synthesis with H_3BTC, a predetermined amount of H_3BTC was dissolved in the initial methanol solution. After gelation, the gel was aged at the same condition for 24 h. The as-dried gel was obtained after solvent exchange with IPA at 60 °C for 3 times, 12 h for each, and then dried at 40 °C for 24 h. The crystalline MgO monolith was obtained by the heat treatment in air.

Table 1 Results of varied volume ratio of methanol to water

$V_{methanol}/V_{water}$ (mL)	Results
0.75/0	Homogeneous particle aggregates with low porosity
0.70/0.05	Homogeneous particles aggregates with high porosity
0.60/0.15	Partly disordered particle aggregates
0.50/0.25	Soft gel (No image)
0.40/0.35	Soft gel (No image)
0/0.75	Macroscopically sedimented precipitates

2.3 Characterization

The structures in the micrometer range of resultant gels were examined by a scanning electron microscope (SEM; JSM-6060S, JEOL, Japan). Nitrogen adsorption-desorption isotherms were obtained using BELSORP-mini II (Bel Japan Inc. Japan). Before the measurement, samples were degassed under vacuum at 200 °C. Specific surface area was calculated using the Brunauar–Emmett–Teller (BET) method, and the pore size distribution in the mesopore regime was calculated from the adsorption branch of the isotherm using the Barrett–Joyner–Halenda (BJH) method.

Thermal evolutions of the as-dried gels were measured by differential thermogravimetric analyzer (TG-DTA; Thermo plus EVO, TG-DTA 8120, Rigaku Co., Japan), at a heating rate of 5 °C min^{-1}, with a continuous air supply at 100 mL min^{-1}. The FT-IR (Fourier transform infrared) spectra were obtained by a FT-IR spectrometer (FT-IR; IRAffinity-1, Shimadzu Co., Japan) using the KBr technique. Samples were dried at 120 °C for 1 h before each FT-IR measurement. Crystal structures of the samples were investigated by an X-ray diffractometer (XRD; RINT Ultima III, Rigaku Co., Japan) using Cu Kα ($\lambda = 0.154$ nm) as an incident beam.

3 Results and discussion

3.1 Effect of solvent and polymer

While keeping the total volume of solvent mixture at 0.75 mL and the amount of PVP at 0.16 g, the morphologies of as-dried gels obtained at varied ratios of methanol to water (Table 1) were investigated. As shown in the SEM images as Fig. 1, although macroscopic gelation was observed, disordered aggregates of platy crystallites with a limited fraction of micrometer-scale pores were formed in the absence of externally added water (Fig. 1a). The gel-phase exhibited spherical and continuous features when prepared with the $V_{methanol}/V_{water}$ ratio of 0.70/0.05. At the

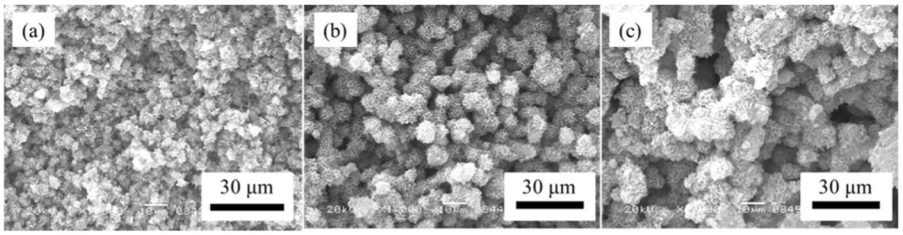

Fig. 1 SEM images of as-dried gels prepared with varied ratios of $V_{methanol}/V_{water}$. **a** 0.75/0; **b** 0.70/0.05; **c** 0.60/0.15. (PVP: 0.16 g)

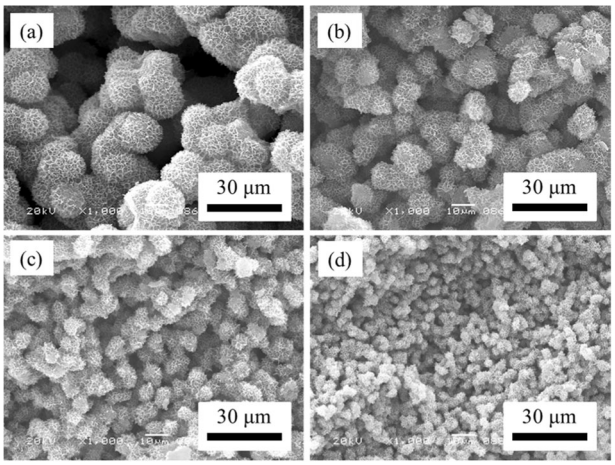

Fig. 2 SEM images of as-dried gels prepared with varied amounts of PVP. **a** 0 g; **b** 0.08 g; **c** 0.16 g; **d** 0.24 g; ($V_{methanol}/V_{water}$: 0.70/0.05)

ratio of 0.60/0.15, the gel-phase became more or less disordered aggregates of spherical units with increased porosity, showing that the structure of resultant gel was sensitively influenced by the composition of the solvent. Gels prepared with 0.50/0.25 and 0.40/0.35 were monolithic but even softer and more fragile than that obtained with 0.70/0.05, and only macroscopic sediment-supernatant phases were obtained when no methanol was used.

Figure 2 shows the SEM images of as-dried gels synthesized with varied amounts of PVP at the $V_{methanol}/V_{water}$ ratio of 0.70/0.05. Even in the absence of PVP, spherical particles aggregated to form a continuous structure (Fig. 2a). With an increase of PVP amount, the size of spherical particles became smaller accompanied by the improvement in homogeneity of the macroporous structure (Figs. 2b–d). The amount of PVP had a weak influence on the gelation time, which indicated that the PVP mainly controlled the phase-separation tendency of the present gelling system.

Divalent magnesium ions are known to exist in an aqueous solution as hexa-aquo complexes in the form of $[Mg(H_2O)_6]^{2+}$. The forced hydrolysis takes place when the pH of the solution is increased, as the equilibrium shown in Eq. 1.

$$[Mg-OH_2]^{2+} \rightleftharpoons [Mg-OH]^{+} + H^{+} \quad (1)$$

Subsequent growth via olation and crystallization into $Mg(OH)_2$ results in the formation of platy hexagons as precipitates. Due to the inherent poor solubility of $Mg(OH)_2$ in water, the essential driving force of phase separation to form the gel-phase is assumed to be the precipitation of $Mg(OH)_2$ out of the aqueous solvent. When nanocrystalline $Mg(OH)_2$, possibly loose aggregates of crystalline particles, are formed in the absence of PVP, at least a part of crystallites can grow freely to form larger platy crystalline precipitates. Since the starting hydrated chloride contains 6 mol of molecular water per Mg, it is possible, even without an external addition of water, for the precursor molecules to form complexes containing multiple hydroxo (Mg-OH) ligands. The rate of formation and aggregation of nanocrystalline $Mg(OH)_2$ rapidly increases with an increase of available water in the solvent phase. If such grown aggregates are tenuous and stay dispersed for an appreciable period of sol–gel reaction, the final product becomes a monolithic gel instead of dispersed or sediment aggregates.

The carbonyl groups in PVP attractively interact with the metal (oxy)hydroxide oligomers through hydrogen bond with M-OH, hindering spontaneous aggregation and growth of crystalline precipitates. In the present system, the platy hexagonal precipitates secondarily aggregated to form spherical gel-phase domains. It is obvious in Fig. 2a, in the $MgCl_2$ $6H_2O$-MeOH-PO system, the formation of monolithic gels is possible without an addition of PVP. The incorporation of PVP is effective in suppressing the secondary growth of spherical crystalline aggregates. The platy habit of the primary crystalline particles, however, remains almost unchanged with additions of PVP in varied concentrations.

3.2 Effect of H_3BTC

Since the growth of nanocrystalline precipitates into larger platy particles leads to the decreased specific surface area of the material, ligands that can suppress the growth of $Mg(OH)_2$ is desired to obtain materials with appreciable specific surface area. With the purpose of preserving fine crystallite size, 1,3,5-benzenetricarboxylic acid, H_3BTC, was utilized, which can form coordinate bonds between its carboxyl groups and Mg ions. With an increased concentration of H_3BTC, both the length and thickness of the

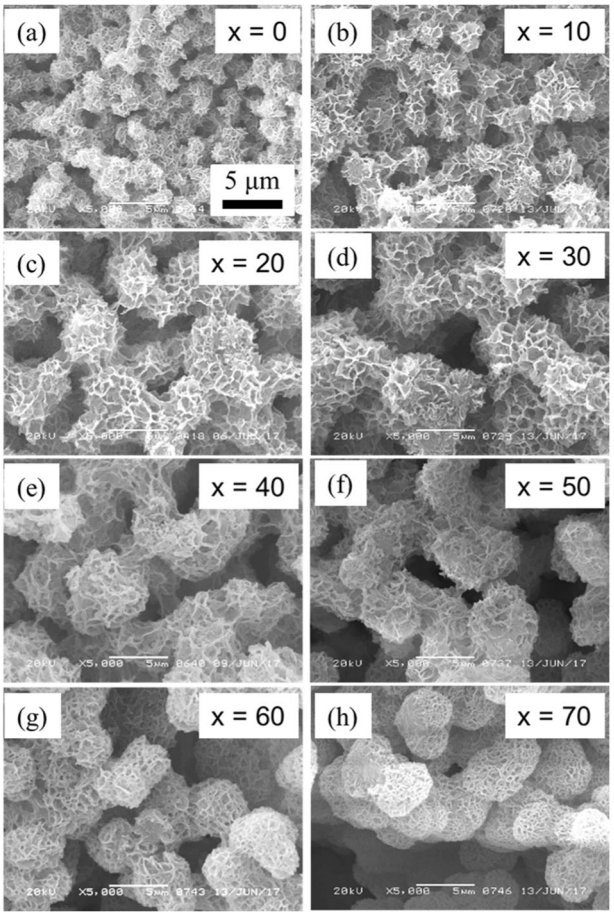

Fig. 3 SEM images of as-dried gels prepared with x μmol of H_3BTC. ($V_{methanol}/V_{water}$: 0.70/0.05; PVP: 0.16 g)

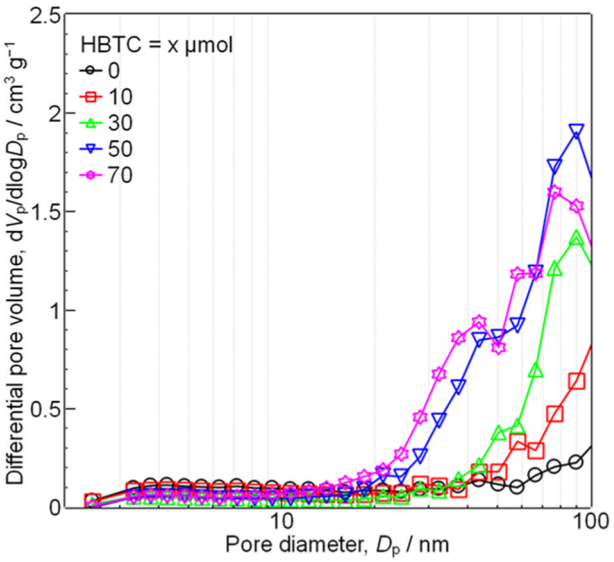

Fig. 4 Pore size distributions of heat-treated samples prepared with varied amounts of H_3BTC. ($V_{methanol}/V_{water}$: 0.70/0.05; PVP: 0.16 g)

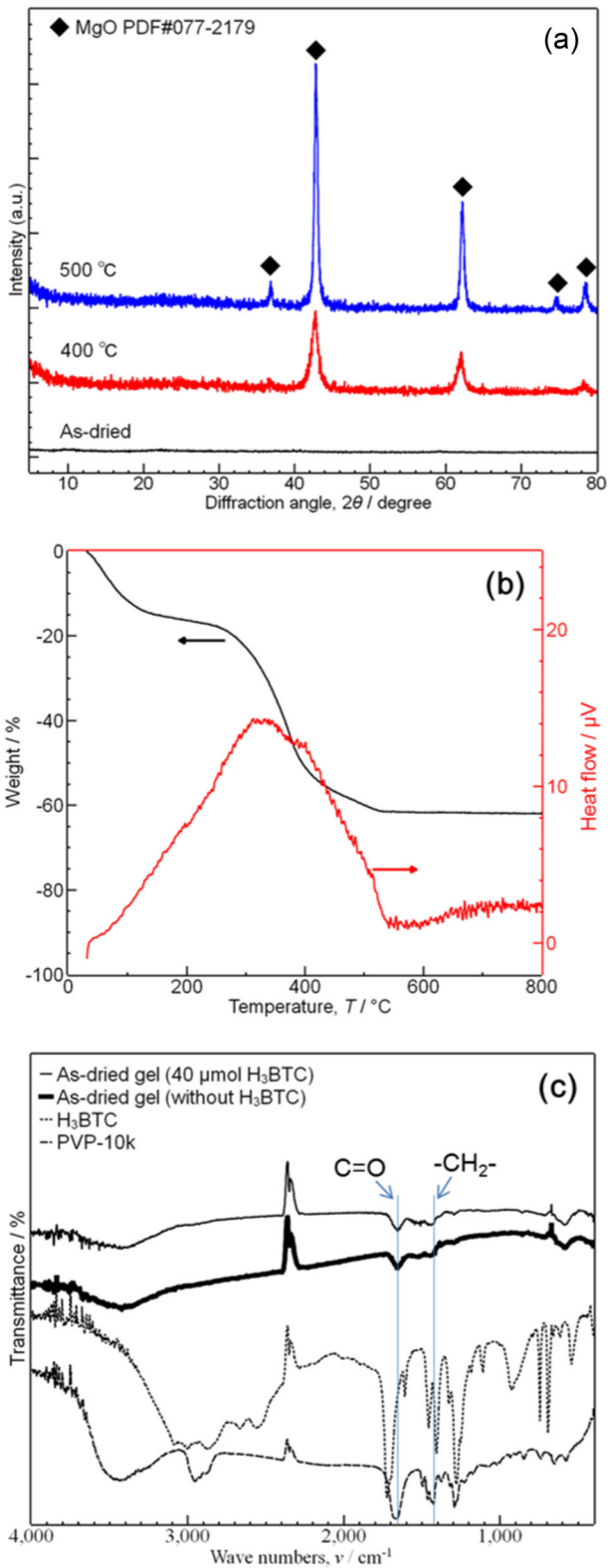

Fig. 5 **a** XRD patterns of as-dried sample and samples heat-treated at varied temperatures; **b** TG-DTA curves of as-dried sample prepared without H_3BTC; **c** FT-IR spectra of as-dried samples prepared in the presence/absence of 40 μmol of H_3BTC. ($V_{methanol}/V_{water}$: 0.70/0.05; PVP: 0.16 g)

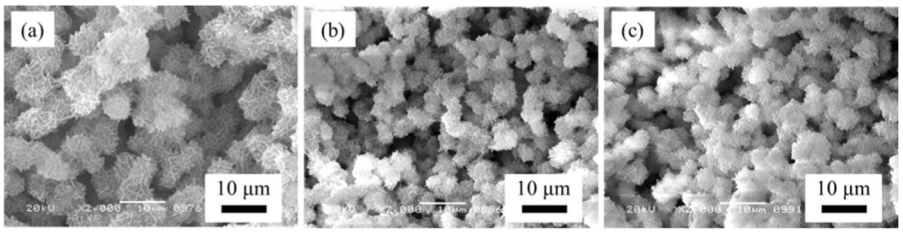

Fig. 6 SEM images of samples after heat treatment at 400 °C (**a**); 500 °C (**b**); 600 °C (**c**). ($V_{methanol}/V_{water}$: 0.70/0.05; PVP: 0.16 g; H_3BTC: 20 μmol)

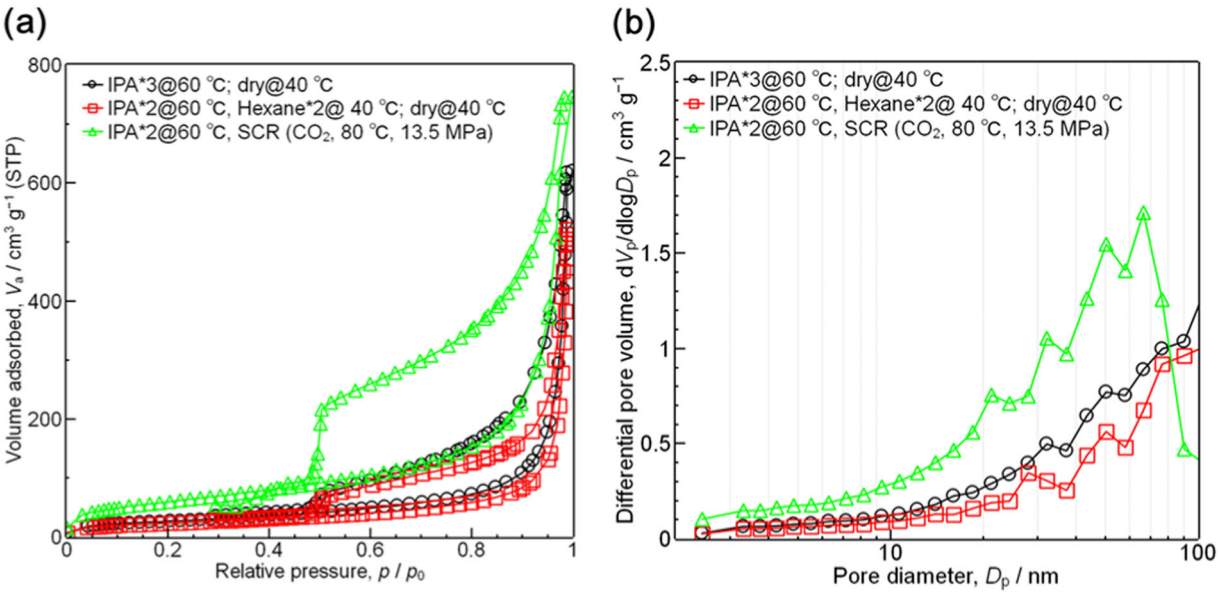

Fig. 7 N_2 adsorption desorption isotherms (**a**) and pore size distributions (**b**) of samples prepared by varied drying processes. ($V_{methanol}/V_{water}$: 0.70/0.05; PVP: 0.16 g; H_3BTC: 20 μmol)

crystalline plates on the surface of skeleton decreased (Figs. 3b–f). The size of spherical aggregates increased gradually with an increase of the H_3BTC accompanied by prolonged gelation time, suggesting that the coordination of H_3BTC to Mg^{2+} ions slowed down the growth of nanocrystalline Mg $(OH)_2$ aggregates. The structures of the samples prepared with varied concentrations of H_3BTC after heat treatment at 500 °C were characterized by nitrogen sorption measurements. The BJH pore size distributions of the gel samples prepared with varied amounts of H_3BTC are shown in Fig. 4. Without H_3BTC, almost no pores were recognized in the mesoporeregion, indicating that most pores have diameters larger than 50 nm. The fraction of pores larger than 30 nm increased with the increasing amount of H_3BTC, in good accordance with the fact that crystalline plates became finer. Other polycarboxylic acids, such as citric acid and tartaric acid, exhibited the similar effects.

3.3 Compositional analysis

Figure 5a shows the XRD patterns of the as-dried gels before and after the heat treatment at varied temperatures. The halo pattern indicates that the as-dried gel is amorphous. The diffraction peaks became evident after heating at 400 and 500 °C. The four intense diffractions at 36.9°, 42.9°, 62.3°, and 78.6° are respectively ascribed to the (111), (200), (220) and (222) crystal planes of MgO (PDF#077-2179), periclase.

The thermal evolutions of as-dried gel prepared without H_3BTC is illustrated in Fig. 5b. About 16% of weight loss was observed at the temperature range below 200 °C, which is attributed to desorption of physically adsorbed water. The 46% of weight loss at the temperature range from 200 to 550 °C accompanied by a broad exothermic peak is ascribed to the combustion of PVP and dehydration of hydroxyl groups. Assuming all initially added Mg atoms remained in the skeleton as MgO, the amount of PVP on/in the skeleton of as-dried gel is ca. 60% of its initial addition. (Here, we ignored that weight loss caused by dehydration of hydroxyl groups, since it accounted for only a small fraction.) Although the mass of MgO accounts for only about 1/3 of the initial solid mass of skeleton, the monoliths did not collapse after the removal of PVP by heating (see Fig. 6). The skeleton is dominantly formed by the Mg–O bond after

Table 2 Properties of samples obtained from varied drying processes and heat treatment temperatures

Sample	BET specific surface area (m^2/g)	BJH pore volume (cm^3/g)
As-dried (SCD)	218	1.07
As-dried (n-hexane)	82	0.79
As-dried (IPA)	96	0.91
Heat-treated (400 °C)	185	1.97
Heat-treated (500 °C)	64	0.97
Heat-treated (600 °C)	48	0.75

the heat treatment, although the mechanical strength decreased substantially.

The FT-IR spectrometer was utilized to examine the chemical structure of the as-dried gels prepared with 0.16 g of PVP and in the presence/absence of 40 µmol of H_3BTC (Fig. 5c). The presence of H_3BTC was not clearly detected by FT-IR. The adsorption bands at around 1660 and 1420 cm^{-1} are attributed to the carbonyl group (C=O) and methylene group (–CH_2–), respectively, indicating that PVP is present on/in the skeleton, which agrees with the result of TG-DTA. The band of carbonyl group in the gel samples showed only a slight shift from that of the free carbonyl group (from 1666 to 1653 cm^{-1}), indicating that the interaction between PVP and the Mg-based particles is relatively weak [20]. Considering the fact that the samples remained monolithic even after the removal of PVP by heat treatment, being different from the cases with HPAA and PAAm, PVP does not work as the main component to mechanically support the continuous Mg-based network.

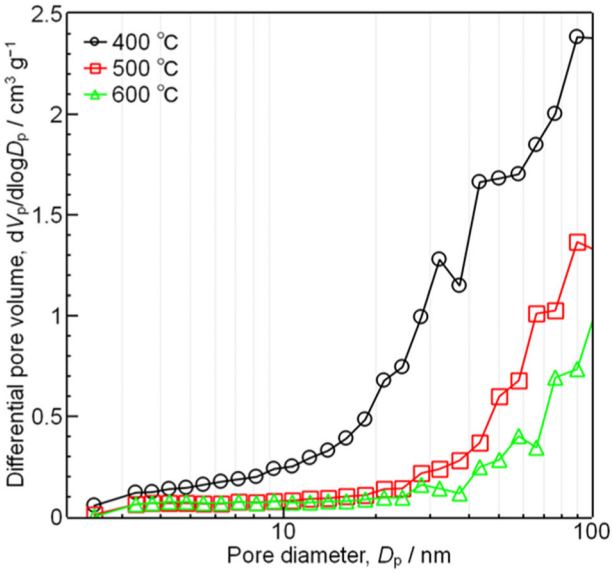

Fig. 8 Pore size distributions of samples after heat treatment at varied temperatures. ($V_{methanol}/V_{water}$: 0.70/0.05; PVP: 0.16 g; H_3BTC: 20 µmol)

3.4 Drying process and heat treatment

Drying of wet gels by evaporation of the pore liquid exerts capillary forces that may cause the collapse of micropores, mesopores and even macropores. Three different processes were examined to remove solvents from the wet Mg-based monoliths; (a) solvent exchange to IPA and drying at 40 °C, (b) solvent exchange to *n*-hexane and drying at 40 °C, (c) supercritical drying after exchange to IPA and to supercritical CO_2 in a pressure chamber. Supercritical drying is considered to be the way that the porous structure of the gel can be preserved to the highest extent.

Figures 7a, b respectively show the nitrogen adsorption-desorption isotherms and the corresponding pore size distributions of the samples prepared with 20 µmol of H_3BTC and dried by the different processes (a)–(c) described above. All the samples exhibited the isotherms of type IV of the IUPAC classification with relatively small uptakes at lower relative pressures. The hysteresis loops of type H3 indicates that the pores are formed as interstices of plate-like particles, which agrees with the SEM results. Figure 7b shows that considerable fractions of micropores and mesopores have collapsed in the samples dried in ambient conditions at 40 °C relative to that dried by supercritical drying. The BET surface area also showed the values consistent with this result (Table 2).

The samples ambient-dried with IPA were used to examine the heat evolution of the nanostructure. It is confirmed from SEM images that the macroporous structures were not damaged after the heat treatment in air at varied temperatures (Fig. 6). However, the shrinkage became noticeable at 500 and 600 °C. Since $Mg(OH)_2$ powders are known to release water on transforming to MgO at around 350 °C, some fraction of the weight loss observed in TG-DTA above 300 °C can be ascribed to the dehydration. About 50% weight loss in the temperature range between 300 and 500 °C well explains the shrinkage also due to the oxidative decomposition of organic components. The Table 2 displays the summary of specific surface area and pore volume of the samples. When the sample was heated to 400 °C, the crystalline structure changed from amorphous to periclase, and most of the organics were removed. These two facts resulted in the increase in specific surface area and pore volume. With a further increase of the heating temperature, the organics were decomposed completely, and the fine MgO

crystals grew further, resulting in the decreased specific surface area and pore volume of the MgO monoliths (Fig. 8).

4 Conclusion

Hierarchically porous MgO monoliths with a well-defined continuous macroporous structure have been prepared via the sol-gel process accompanied by phase separation. The macropore structure can be controlled by the ratio of water to methanol and the amount of PVP, which acted as not only a phase separation controller but also a component to reinforce the Mg-based network. After the heat treatment in air, the macroporous structure was preserved without serious damage. A polycarboxylic acid, H_3BTC, was employed to hinder the growth of precipitated crystalline particles. The addition of H_3BTC leads to the increase of specific surface area of the monoliths. These results suggest a possible way to synthesize monolithic divalent metal oxides with high specific surface area.

Acknowledgements The present study has been performed under financial supports from Advanced Low Carbon Technology Research and Development Program (ALCA, Japan Science and Technology Agency).

Compliance with ethical standards

Conflict of interest The authors declare that they have no conflict of interest.

References

1. Shi L, Chu Z, Liu Y, Jin W, Xu N (2014) In situ fabrication of three-dimensional graphene films on gold substrates with controllable pore structures for high-performance electrochemical sensing. Adv Funct Mater 24:7032–7041
2. Collins G, Blomker M, Osiak M, Holmes JD, Bredol M, O'Dwyer C (2013) Three-dimensionally ordered hierarchically porous tin dioxide inverse opals and immobilization of palladium nanoparticles for catalytic applications. Chem Mater 25:4312–4320
3. Tanaka N, Nagayama H, Kobayashi H, Ikegami T, Hosoya K, Ishizuka N, Lubda D (2000) Monolithic silica columns for HPLC, micro-HPLC, and CEC. J Sep Sci 23:111–116
4. Srinivas G, Krungleviciute V, Guo ZX, Yildirim T (2014) Exceptional CO_2 capture in a hierarchically porous carbon with simultaneous high surface area and pore volume. Energy Environ Sci 7:335–342
5. Nakanishi K, Soga N (1991) Phase separation in gelling silica-organic polymer solution: systems containing poly (sodium styrenesulfonate). J Am Ceram Soc 74:2518–2530
6. Flory PJ (1942) Thermodynamics of high polymer solutions. J Chem Phys 10:51–61
7. Huggins ML (1942) Some properties of solutions of long-chain compounds. J Phys Chem 46:151–158
8. Konishi J, Fujita K, Nakanishi K, Hirao K (2006) Monolithic TiO_2 with controlled multiscale porosity via a template-free sol-gel process accompanied by phase separation. Chem Mater 18:6069–6074
9. Hasegawa G, Kanamori K, Nakanishi K, Hanada T (2010) Facile preparation of hierarchically porous TiO_2 monoliths. J Am Ceram Soc 93:3110–3115
10. Konishi J, Fujita K, Oiwa S, Nakanishi K, Hirao K (2008) Crystalline ZrO_2 monoliths with well-defined macropores and mesostructured skeletons prepared by combining the alkoxy-derived sol–gel process accompanied by phase separation and the solvothermal process. Chem Mater 20:2165–2173
11. Tokudome Y, Fujita K, Nakanishi K, Miura K, Hirao K (2007) Synthesis of monolithic Al_2O_3 with well-defined macropores and mesostructured skeletons via the sol–gel process accompanied by phase separation. Chem Mater 19:3393–3398
12. Schubert U, Hüsing N (2012) Synthesis of inorganic materials. CPI Group Ltd, Croydon, UK, Chapter 4
13. Gash AE, Tillotson TM, Satcher Jr JH, Poco JF, Hrubesh LW, Simpson RL (2001) Use of epoxides in the sol-gel synthesis of porous iron (III) oxide monoliths from Fe (III) salts. Chem Mater 13:999–1007
14. Baumann TF, Gash AE, Chinn SC, Sawvel AM, Maxwell RS, Satcher JH (2005) Synthesis of high-surface-area alumina aerogels without the use of alkoxide precursors. Chem Mater 17:395–401
15. Kido Y, Nakanishi K, Miyasaka A, Kanamori K (2012) Synthesis of monolithic hierarchically porous iron-based xerogels from iron (III) salts via an epoxide-mediated sol-gel process. Chem Mater 24:2071–2077
16. Kido Y, Nakanishi K, Okumura N, Kanamori K (2013) Hierarchically porous nickel/carbon composite monoliths prepared by sol-gel method from an ionic precursor. Microporous Mesoporous Mater 176:64–70
17. Kido Y, Hasegawa G, Kanamori K, Nakanishi K (2014) Porous chromium-based ceramic monoliths: oxides (Cr_2O_3), nitrides (CrN), and carbides (Cr_3C_2). J Mater Chem A 2:745–752
18. Fukumoto S, Nakanishi K, Kanamori K (2015) Direct preparation and conversion of copper hydroxide-based monolithic xerogels with hierarchical pores. New J Chem 39:6771–6777
19. Gash AE, Satcher Jr JH, Simpson RL (2004) J Non-Cryst Solids 350:145–151
20. Liu M, Yan X, Liu H, Yu W (2000) An investigation of the interaction between polyvinylpyrrolidone and metal cations. React Funct Polym 44:55–64